Phase Transitions of PYR_{14}-TFSI as a Function of Pressure and Temperature: the Competition Between Smaller Volume and Lower Energy Conformer.

F. Capitani[1], F. Trequattrini,[1,2] O. Palumbo,[2] A. Paolone[2], P. Postorino,[1,*]

[1] Dipartimento di Fisica, Sapienza Università di Roma, Piazzale A. Moro 5, 00185 Rome, Italy

[2] CNR-ISC, U.O.S. La Sapienza, Piazzale A. Moro 5, 00185 Rome, Italy

Abstract

A detailed Raman study has been carried out on the ionic liquid 1-butyl-1-methylpyrrolidinium bis(trifluoromethanesulfonyl)imide (PYR_{14}-TFSI) over a wide pressure (0-8 GPa) and temperature (100-300 K) range. The explored thermodynamic region allowed us to study the evolution of the system across different solid and liquid phases. Calculated Raman spectra remarkably helped in the spectral data analysis. In particular, the pressure behavior of the most intense Raman peak and the shape analysis of the ruby fluorescence (used as a local pressure gauge) allowed us to identify a liquid-solid transition around 2.2 GPa at T=300 K. Low frequency Raman signal as well as the absence of remarkable spectral shape modifications on crossing the above threshold and the comparison with the spectra of the crystalline phase, suggest a glassy nature of the high pressure phase. A detailed analysis of the pressure dependence of the relative concentration of two conformers of TFSI allowed us to obtain an estimate of the volume variation between *trans*-TFSI and the smaller *cis*-TFSI which is the favored configuration on applying the pressure. Finally, the combined use of both visual inspection and Raman

[*]Corresponding author: Paolo Postorino, Dipartimento di Fisica, Sapienza Università di Roma, Piazzale A. Moro 5, I-00185 Rome, Italy e-mail: Tel. +39 06 4991 3502 - Fax +39 06 4463158

spectroscopy confirmed the peculiar sequence of phase transitions observed as a function of temperature at ambient pressure and the different spectral/morphological characteristics of the two crystalline phases.

Introduction

Ionic liquids (ILs) are inorganic salts with melting point below 100 °C and many of them are liquid even below room temperature. They have attracting properties such as very large liquids ranges, low volatility, high conductivity and the ability to solubilize a broad variety of materials which make them good candidates as green solvents. ILs have been largely studied for their possible use in a wide range of areas including catalysis and electrochemistry.[1,2] Moreover, their properties can be tuned by variation of the cation and anion.

The low melting temperatures are fundamentally determined by the steric hindrance due to the large dimensions of the composing ions, since increasing the size of the ions decreases ion-ion interactions and prevents efficient packing of the ions into a crystal structure.[1] The liquid structure is characterized by a balance between long-range Coulomb electrostatic forces among the constituent ions and local geometric factors.[3,4] As the temperature is decreased, they usually crystallize displaying plastic solid phases which originate in the rotational disorder present in the crystals. Indeed, the ions which compose the ILs are not spherical and can be arranged in various ordered or disordered geometries in the crystal structures.[2] Moreover, by setting proper change of temperature, many ILs can enter a supercooled regime or form glasses.[2,5]

The remarkable technological interest for these materials asks for a full understanding of their macroscopic properties and their dependence on the microscopic molecular structure and dynamics; therefore a growing body of information on ionic liquids has been obtained from the combined use of several spectroscopic techniques.[1,2,6,7] Among them, Raman spectroscopy provides information on important structural features of ionic liquids,[6,7] such as anion-cation interactions,[8] liquid-solid transitions,[9] hydrogen bonding,[9-12] conformation of alkyl chains,[13] or ionic pair formation in solutions of lithium salts in ionic liquids.[14] In

these high-frequency Raman studies of ionic liquids, as well as in infrared spectroscopy studies, the assignment of vibrational modes might be achieved by comparison with quantum chemical calculations.[7,9-12,15] Low-frequency Raman spectra, typically below 200 cm^{-1}, show a common behavior resulting from a broad intermolecular vibrational dynamics (the boson peak, and relaxation processes).[7,16,17] Indeed, the low frequency broad features have been assigned to collective modes of local structures with different size, in particular the Gaussian components have been assigned to the inhomogeneously broadened bands due to collective motions of cations involved in local structures.[17]

Moreover, systematic temperature and pressure dependent Raman spectroscopy studies focused on the occurrence of liquid-solid and solid-solid transitions and on the nature of the intermolecular interactions.[3,4,6-8] Indeed, the exploration of an extended *p*-*T* region allows to draw general remarks on the phase diagram of ILs.[6] On the other hand, the use of pressure is a clean tool for a fine tuning of the strength of intermolecular interactions without the unavoidable perturbations and side effects when exploiting changes in temperature and chemical composition.[3,4] In particular, applying pressure mainly induces density changes, whereas temperature varies both activation energy and density.[3,4] The volume compression reduces the average distances among the ionic charges thus enhancing the direct Coulomb interaction, with a possible competition with the steric hindrance of both cation and anion.[6]

For instance, in analogy with cold crystallization usually observed when supercooled ionic liquids are re-heated, high pressure Raman experiments showed that two different ionic liquids based on the $(BF_4)^-$ anion can be pressurized above 5.0 GPa at room temperature, undergoing crystallization after releasing the pressure below $\sim$2.0 GPa.[3,4,18-20] Other studies detected below 1.0 GPa the presence of liquid-crystal and crystal phase transitions of imidazolium based ILs, having different anion, i.e. Cl^-, Br^- and PF_6^-.[21,22]

An interesting difference was reported[3,4,23] between the behavior under high pressure of two ionic liquids sharing the same cation (N,N-diethyl-N-methyl-N-(2-methoxyehtyl)ammonium), but having different anions (bis(trifluoromethylsulfonyl)imide (TFSI) and tetrafluoroborate (BF_4^-)): no crystallization was observed for the TFSI based liquid up to 4.3 GPa, whereas crystallization of the BF_4^- based liquid was observed already at 1.4 GPa. Most probably, the complex molecular structure of the TFSI anion, with several conformations allowed, is hindering crystallization within the explored pressure range. Moreover, a high pressure Raman study[23] focused on 1-butyl-1-methylpyrrolidinium – TFSI (PYR_{14}-TFSI); in particular, the authors follow the linear frequency shift of few lines between 690 and 750 cm^{-1} and no crystallization was observed up to 4 GPa.

In the present work we carried out a systematic and detailed Raman study of PYR_{14}-TFSI, as a function of either pressure or temperature, exploring a relevant part of its phase diagram. This liquid has been widely studied for its possible use in green and safe electrolyte systems[1,2,5] but a complete high pressure study is still lacking.

Experimental

The ionic liquid 1-butyl-1-methylpyrrolidinium bis(trifluoromethanesulfonyl)imide PYR_{14} - TFSI was purchased from Solvionic. As the purity was higher than 99.9%, the sample was investigated as received without further purification.

The Raman spectra were measured with a Horiba LabRAM HR Evolution microspectrometer in backscattering geometry. Samples were excited by the 632.8-nm radiation of a He-Ne laser with 30 mW output power. The elastically scattered light was removed by a state-of-the-art optical filtering device based on three BragGrate notch filters.[24] Raman spectra were collected by a Peltier-cooled charge-coupled device (CCD)

detector with a ultimate spectral resolution which can be better than 1 cm^{-1} thanks to a grating with 1800 grooves/mm with a 800-mm focal length. Measurements over the 10–1000 cm^{-1} range were performed using a long-working-distance 20X objective. For the temperature dependent measurements the sample was contained in a small hole (few mm^3) drilled in a copper slab mounted on the cold finger of a liquid-nitrogen-cooled horizontal cryostat by Oxford Instruments. Measurements were carried out over the 80–300 K temperature range and our thermoregulation setup allowed a thermal stability within ± 2 K during data collection at each working temperature.

For the pressure dependent measurements the sample was pressurized using a diamond anvil cell from BETSA equipped with low fluorescence IIA diamonds with a culet of about 800 μm. The sample was loaded in a hole (250 μm diameter and 50 μm height under working conditions) of a Mo gasket originally 250 μm thick. The ruby fluorescence technique has been exploited for in situ pressure measurement. Exploiting a camera mounted on the microscope, images of the sample under pressure have been collected to verify the occurrence of liquid-solid transitions also by a simple visual inspection.[25] Further experimental details for the temperature and the pressure Raman setups can be found in Refs. 26 and 27, respectively.

Computational

Starting from the known conformation of TFSI and PYR_{14}, we obtain the optimized geometries of *cis*- and *trans*-TFSI and of lowest energy conformer of PYR_{14} (formally the equatorial-envelope conformer) by means of the Firefly package, using the 6-31G ** basis set and B3LYP theory, as largely performed in the previous literature. The Raman vibration frequencies and activities ($Å^4$/amu) were calculated by the same software. In

order to compare the experimental Raman spectrum with the calculated one, we constructed an expected Raman spectrum summing Lorentzian curves centered at each calculated Raman frequency, with an intensity proportional to the calculated one and a fixed line width of 10 cm^{-1}.

Results and Discussion

Computational results: a preliminary attribution of the experimental Raman bands

The optimized geometries of *trans*- and *cis*-TFSI and of the equatorial-envelope conformer of PYR_{14} are reported in Fig. S1 of the Supporting Info. The calculated Raman vibration frequencies and activities ($Å^4$/amu) are reported in Table S1.

In Fig. 1 we report a comparison of the experimental spectrum of PYR_{14}-TFSI at room temperature and pressure, with the calculated Raman spectra of the PYR_{14} and of the two conformers of TFSI. For the pyrrolidinium ion no scaling factor was used, while for the two TFSI conformer a scaling factor 1.05 was applied, in agreement with the previous literature.[28-30] As expected, there is a general good agreement between the experiment and the calculated frequencies of vibrations of single ions. The previous literature and the here repeated calculations suggest that some Raman bands can be used to distinguish between the occurrence of the *trans* or *cis* conformer of TFSI: in particular the line centered around 742 cm^{-1} is the sum of two contribution from *cis*- and *trans*-TFSI separated by 3 cm^{-1}. Despite the large intensity of makes this band attractive, in the present study we recorded the experimental spectra with a resolution of 2-3 cm^{-1}, and therefore we avoided to use this line to study the conformer concentration. The bands centered around 630 and 653 cm^{-1} are known to be due to *trans*- and *cis*-TFSI respectively. However, calculations suggest the occurrence of superimposed bands due to

PYR_{14} having a comparable Raman activity. The series of lines centered in the frequency range between 250 and 370 cm^{-1} seem to be the best candidates for an investigation of the presence of TFSI conformers. The bands at 279, 298 and 313 cm^{-1}, together with the shoulder at 288 cm^{-1} contain contributions from both conformers and even from PYR_{14}; however, the bands at 327 and 340 cm^{-1} are clearly attributable to *cis* and *trans*-TFSI, respectively. Moreover, the shoulder at 351 cm^{-1} is due to the *cisoid* conformer. Finally one can note that the band around 210 cm^{-1} is mainly due to *cis*-TFSI, while all the bands between 820 and 1100 cm^{-1} are due to vibrations of the cation. These attributions are in agreement with previous studies of the Raman spectra of some TFSI based ionic liquids.[3,21]

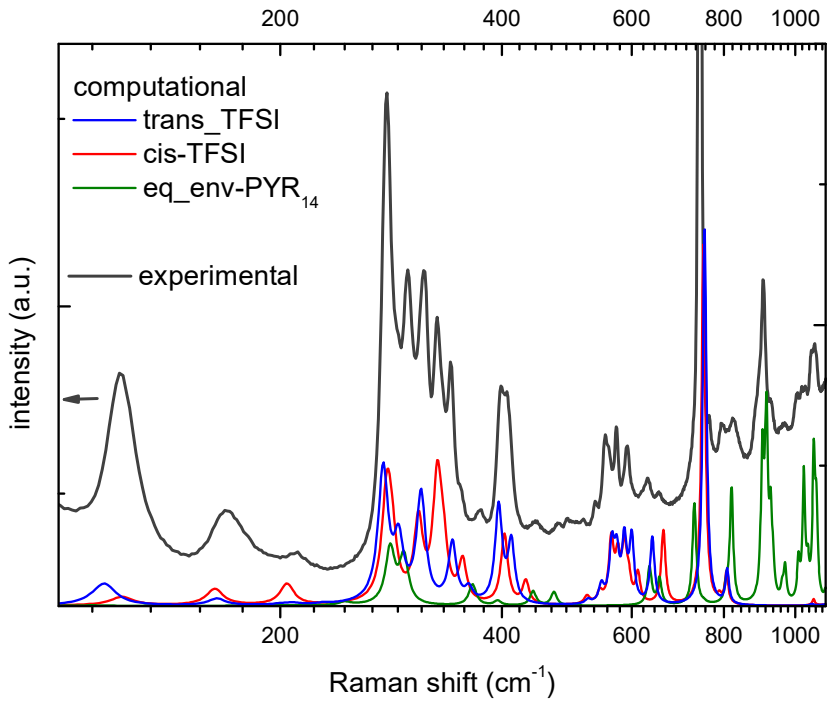

Fig. 1 Experimental Raman spectrum of PYR_{14}-TFSI at room temperature compared with the calculated Raman spectra of *trans*- and *cis*-TFSI and PYR_{14}. For the pyrrolidinium ion no scaling factor was used, while for the two TFSI conformer a scaling factor 1.05 was applied.

Raman spectrum as a function of temperature

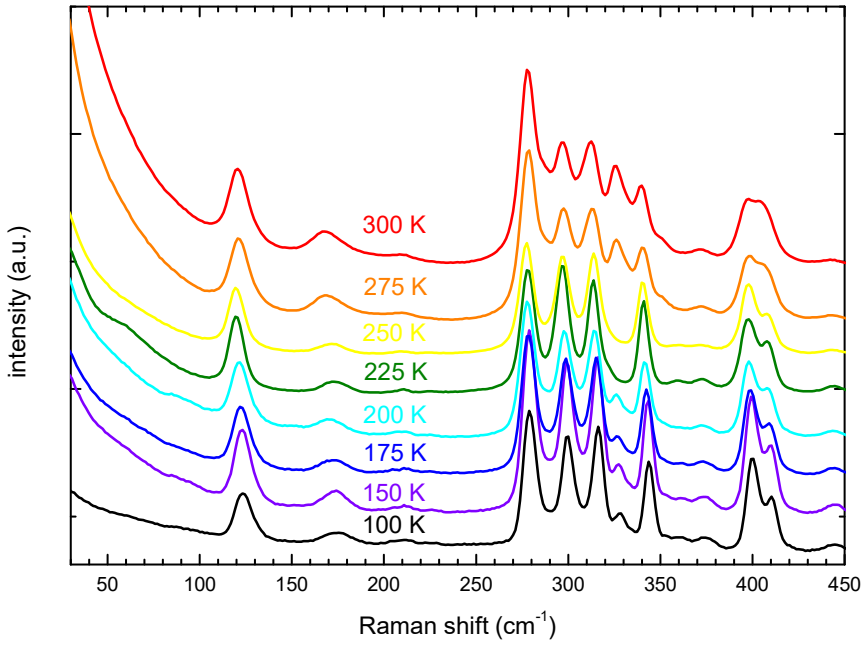

Fig. 2 Temperature dependence of the Raman spectrum of PYR_{14}-TFSI in the frequency range 30-450 cm^{-1}. The spectra are vertically shifted for clarity.

As already reported, after cooling, PYR_{14}-TFSI undergoes a series of phase transitions during heating:[2] the IL undergoes a devitrification transition around 190 K, passing to a super cooled liquid phase. Around 217 K PYR_{14}-TFSI becomes a crystalline solid, but on further heating it undergoes a solid-solid phase transition around 241 K. Finally above ~ 268 K it becomes liquid (see Fig. S2 of the Supporting Info). Raman spectra of PYR_{14}-TFSI over two relevant spectral ranges are shown in Fig. 2 and Fig. 3 as a function of temperature. As expected, the linewidth of Raman peaks slightly increases on heating albeit a close inspection of the spectra at 225 K and 250 K (i.e. in the crystalline phases I and II) shows a detectable reduction of the linewidth, see for example the peak around 900

cm^{-1} in Fig. 3. As to the expected frequency softening of the peaks on heating, we notice that the most intense peak moves from 747 cm^{-1} (100 K) to 743 cm^{-1} (300 K) (see inset of Fig. 3). The most striking changes as a function of T are shown by the band centered around 327 cm^{-1} (see Fig. 2), which has been attributed to a vibration of *cis*-TFSI. Indeed this band completely disappears in the spectra measured at 225 and 250 K, i.e. in the two solid phases of PYR_{14}-TFSI. A similar behavior is also displayed by the band centered around 210 cm^{-1}, which has a strong component due to *cis*-TFSI. Both features are consistent with a suppression of *cis*-TFSI in the solid phases of the ionic liquid. Indeed, an X-ray diffraction study reported that[31] in the solid phase the sample has an orthorhombic $P2_12_12_1$ structure containing only *trans*-TFSI.[30] However, this study did not investigate the differences between the two solid phases. The *transoid* is the lowest energy conformer of TFSI and in many ionic liquids only this rotamer is retained in the solid phases,[3,32] even though there are some exceptions.[32,33] Moreover, the onset of the crystalline phases is also marked by the appearance of a broad peak around 60 cm^{-1} which can be ascribed to intermolecular vibrational modes activated in the crystalline phase.

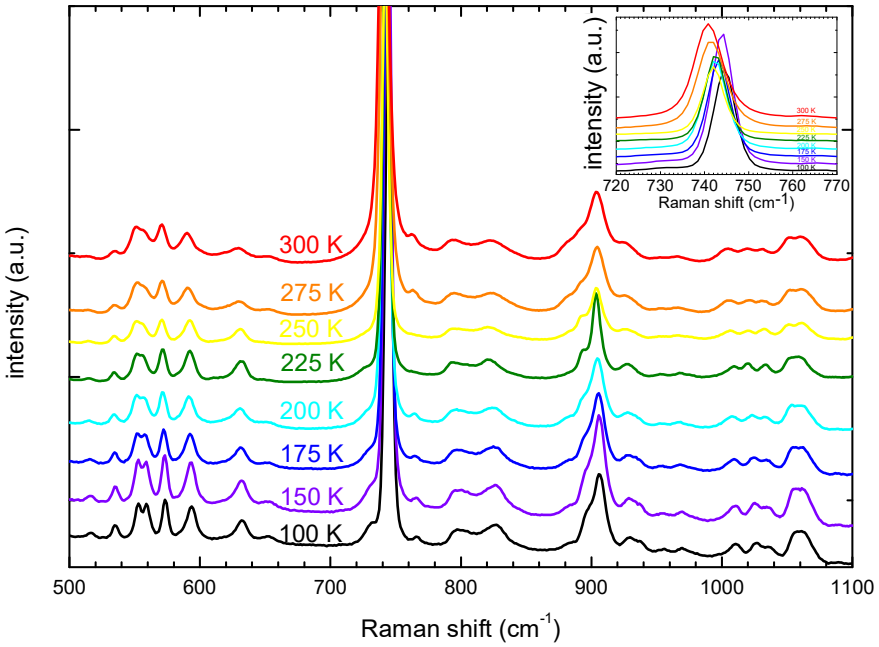

Fig. 3 Temperature dependence of the Raman spectrum of PYR_{14}-TFSI over the 500-1100 cm^{-1} frequency range. The spectra are vertically shifted for clarity.

The sequence of phases exhibited by the system on increasing the temperature can be also revealed by the visual inspection of the sample within the copper container placed on the cold finger of the cryostat. At 150 K the system is in a glassy state, the solid is fully transparent although several cracks are clearly visible in Fig. 4a. As the temperature is increased, cracks gradually disappear and the system undergoes a devitrification transition up to 200 K (see fig. 4b). On further heating the system passes through two crystalline phases (labeled as I and II) characterized by completely different morphologies: at 225 K, phase I shows round-shaped crystalline domains of the dimension of tens of micrometers, whereas the domains of phase II at 250 K are needle-like. Further temperature increase leads the sample to the original liquid phase.

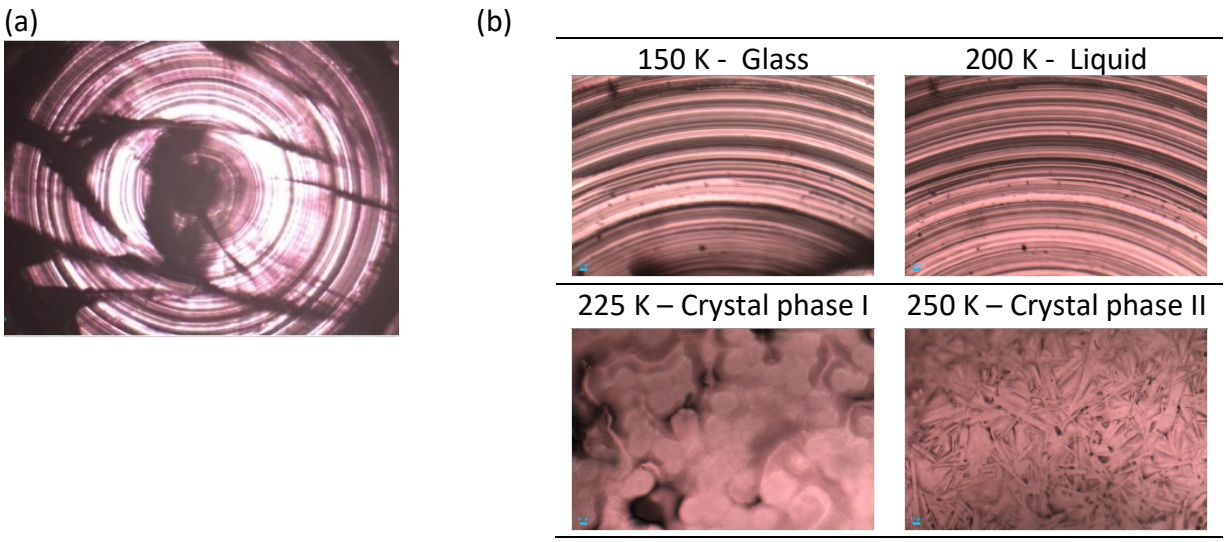

Figure 4: (a) Image of the sample within a copper container at 150 K. The image has been collected with a 4x objective. The diameter of the container is about 2 mm. (b) Images of the sample within a copper container at four selected temperatures on heating. Images have been collected with a 20x objective. Concentric circles clearly visible when the system is transparent (i.e. in (a) and in the first two images of (b)) are simply due to the manufacturing of the copper container and are not related with the sample morphology.

Raman spectrum as a function of pressure

The pressure dependence of the Raman spectrum of PYR_{14}-TFSI measured at 300 K is reported in Fig. 5.

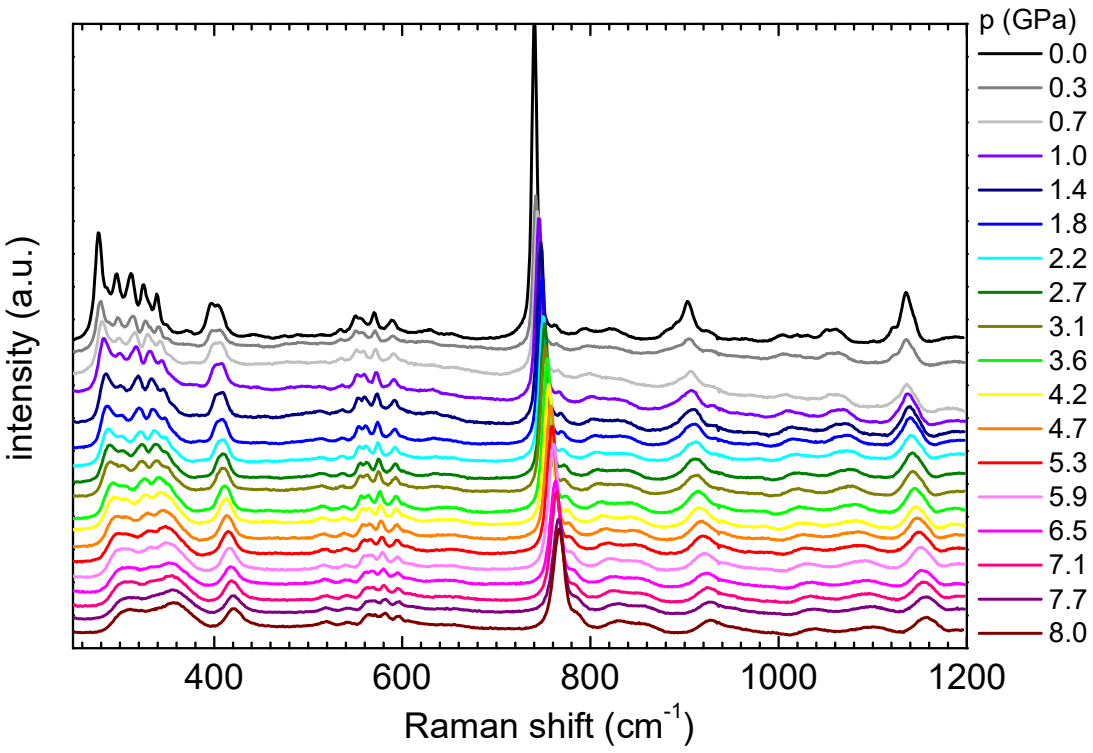

Fig. 5 Pressure dependence of the Raman spectrum of PYR_{14}-TFSI in the frequency range 250-1200 cm^{-1}. The spectra are vertically shifted for clarity.

The overall shape of the Raman spectrum does not remarkably changes under compression although, as expected, most of the lines broaden and shift towards higher frequencies on increasing the pressure. Looking at Fig. 5, the most important effect induced by increasing the pressure is the progressive spectral shape modification of the large multiband feature within the 250-370 cm^{-1} frequency range. By comparing Fig. 2 (T-behavior) with Fig. 5 (P-behavior) completely different trends are observed. The overall modification of this peculiar multiband spectral structure as a function of increasing pressure can be seen indeed as the combined effect of a progressive enhancement of the cis-TFSI peak (around 327 cm^{-1} at 0 GPa) and of a sensible line-shape broadening. As a function of temperature (at P=0) we recall that the cis-TFSI peak disappears when the crystalline phases are established at 225 K and 250 K (see Fig. 2) and, at any

temperature, its intensity does never stand above the other peaks of the multiband structure as it does at the highest pressures (see Fig. 5.)

These findings indicate that the compressed system does not enter any of the crystalline phases obtained at low temperatures but, if pressure induces a solid phase, this should somehow preserve the disordered character of the liquid. Also in analogy to the lowest temperature phase observed, a pressure induced transition to glassy state can be conjectured. A closer inspection of the data and a careful data analysis are however needed to search for a possible liquid-solid transition under pressure as well as to investigate the nature of the solid phase.

The pressure dependence of the central frequency of the most intense Raman band, ν_{MAX}, centered around 740 cm^{-1} at p = 0 GPa, is shown in Fig. 6. It is evident that the band broadens and shifts at higher frequency on increasing p; however, one can note two different linear dependences with a slope, $d\nu_{MAX}/dp$, of about 4.7 cm^{-1}/GPa at low pressure and $d\nu_{MAX}/dp$ = 2.9 cm^{-1}/GPa at high pressures. The change between the two slopes is rather abrupt and it occurs at around 2 GPa. Our results are in agreement with a previous work[23] about the pressure dependence this line in PYR_{14}-TFSI extending only up to 4 GPa, that showed a deviation from the linear one between 2 and 3 GPa.

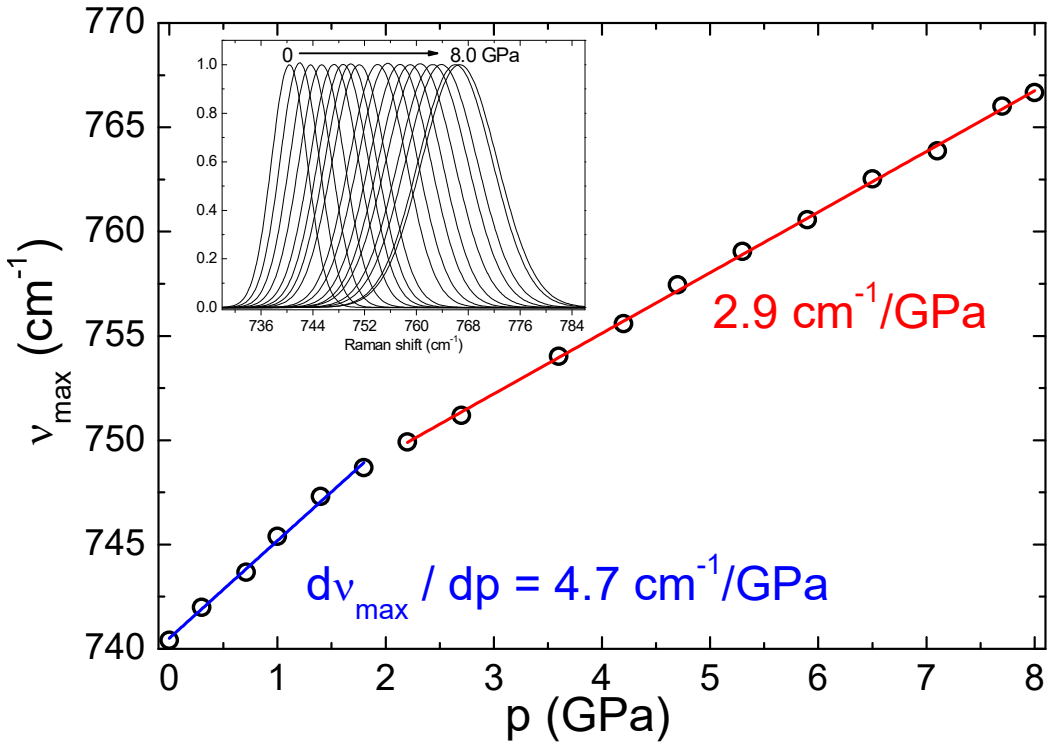

Fig. 6 Dependence on pressure of the frequency of the maximum of the intense band centered around 740 cm^{-1} at *p* = 0 GPa. Colored lines are the best fit curves below and above 2 GPa. In the inset, the experimental spectrum of the normalized band is reported as a function of pressure.

Anomalies at around the same pressure can be observed also looking at the shape of the fluorescence signal collected from the ruby microspheres used as pressure sensors. It is known indeed that the shape of the fluorescence signal provides information about the sample hydrostatic conditions. In particular, pressure induced liquid-solid transition (thus a transition to a less hydrostatic environment) can be clearly detected by the abrupt increase of the bandwidth Γ(p) of the R1 ruby fluorescence line. Piermarini et al.[34-35] indeed showed that such a broadening is the direct consequence of the occurrence of non-hydrostatic stresses. The method proposed in Refs. 34-35 can be thus exploited to determine the solidification transition pressure. This has been indeed applied to glass-formers and, more

recently, also for ionic liquids.[3,4,17] Following this idea, we analyzed the ruby fluorescence signal at each working pressure by a fitting procedure using two Lorentzian functions to describe the two lines. We calculated the difference between the Lorentzian width of the R1 line at a given pressure, Γ(p), and its value at ambient pressure, Γ(0). The pressure dependence of this difference is reported in Fig. 7: it keeps constant up to about 2.2 GPa whereas, at higher pressures, the difference linearly increases. Accordingly with previous findings, P=2.2 GPa can be assumed as the glass formation pressure threshold.

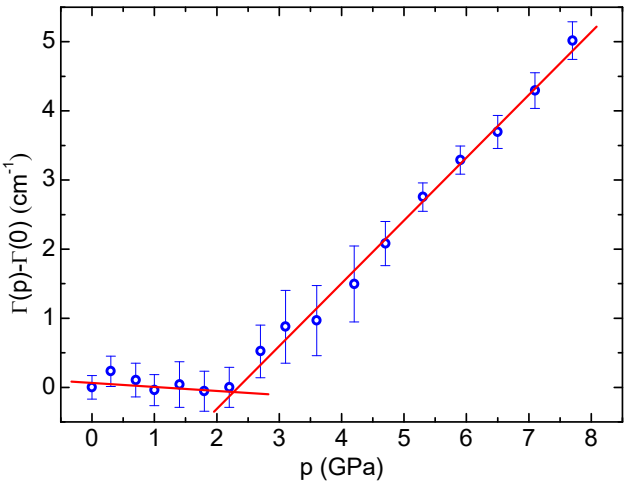

Fig. 7 Pressure dependence of the difference between the width of the ruby R1 fluorescence line at a given pressure p and the width value at 0 GPa. The red lines are guides to the eye.

The transition to a glassy state is also supported by the pressure induced changes in the low frequency region of the Raman spectrum. The spectral range 20-200 cm^{-1} is shown in Fig. 8, where spectra have been shifted in order to have the same intensity value at 100 cm^{-1}. On increasing the pressure up to 2.2 GPa, the intensity of the signal below 100 cm^{-1} decreases, whereas in the 2.2-8 GPa pressure range it keeps almost constant (spectra collected above 3.6 GPa and below 8 GPa are not shown). It is worth noting that

also the shape of the quasi-elastic signal below 50 cm^{-1} changes on increasing pressure. The pressure effect on the shape of the spectra in the low-frequency region can be better appreciated using the Raman susceptibility $\chi(\omega) = I(\omega)/(1 + n(\omega))$, where $I(\omega)$ is the Raman intensity and $n(\omega) = (e^{-\beta\hbar\omega} - 1)^{-1}$ is the thermal population factor.[7,16,17,36] The susceptibility plot is reported in the inset of Fig. 8. The intensity reduction and the blue shift of the band below 100 cm^{-1} is now apparent between 0 and 2.2 GPa, whereas above this pressure value the band shape and position does not change anymore. Since this broad band is related to the intermolecular motion,[7,16,17,36] its pressure dependence points out a hindered molecular motion with almost stuck molecules not responding to the application of an external pressure above 2.2 GPa, consistently with the glass formation.

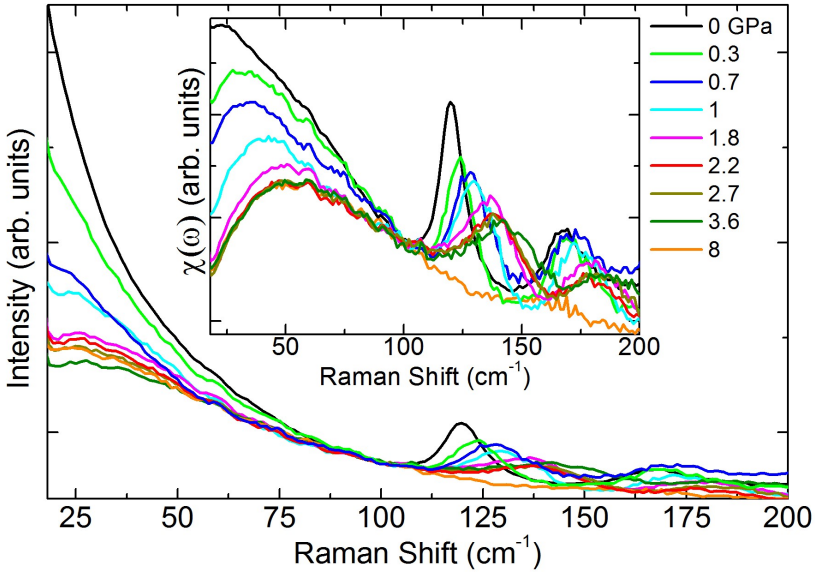

Fig. 8 Pressure dependence of the Raman spectra within the 20-200 cm^{-1} frequency region. The Raman susceptibility plot of the same spectral range is reported in the inset.

The abrupt change of slope in the linear pressure dependence of the main Raman peak (see Fig. 6) and the shape analysis of the ruby fluorescence (see Fig. 7) thus clearly show a sharp pressure induced transition to a solid phase at 2.2 GPa. On the other hand, the

absence of remarkable spectral modifications on crossing the pressure threshold (see the spectra above and below 2.2 GPa in Fig. 5) and the low-frequency Raman signal (see Fig. 8) coherently indicate a glassy nature of the new high pressure solid phase.

We also performed Raman measurements on releasing the pressure (not shown) in order verify the occurrence of crystallization processes, as already observed for other ionic liquids.[3,4,18-20] However, no crystal phases were observed with the system coming back to its original liquid state when the pressure was fully released.

Another aspect of this study regards the investigation of the dependence of the concentration of the two conformers of the TFSI ion on *p*. Indeed, previous studies reported that the ratio of the conformer concentration, *r*, is proportional to the ratio of the intensities of the spectral lines attributable to specific conformers:

$$r = \frac{[C_{cis}]}{[C_{trans}]} = \frac{I_{cis}}{I_{trans}} \quad (1)$$

where I_x designates the integrated intensity of the Raman band centered at wavenumber x,[13] after subtraction of a linear background from the spectra.

For the measurements as a function of pressure, we can use eq. (1) to study the pressure dependence of the concentration of the TFSI conformers. As reported in the section about the attribution of the Raman lines to specific vibrations, the bands which can be attributed to *trans*- and *cis*-TFSI are those centered around 339 and 325 cm^{-1}, respectively, at *p* = 0 GPa. We performed a fit of the Raman spectrum in the frequency range between 260 and 380 cm^{-1} (see Fig. 9) by means of seven Gaussians contributions. Fig. 10 displays ln (*r)*, obtained from the fit, vs. *p* up to 3 GPa, i.e. up to the pressure at which it is still be possible to clearly separate the various bands in the spectrum. It is well evident that the concentration of the *cis*-conformer increases as pressure increases.

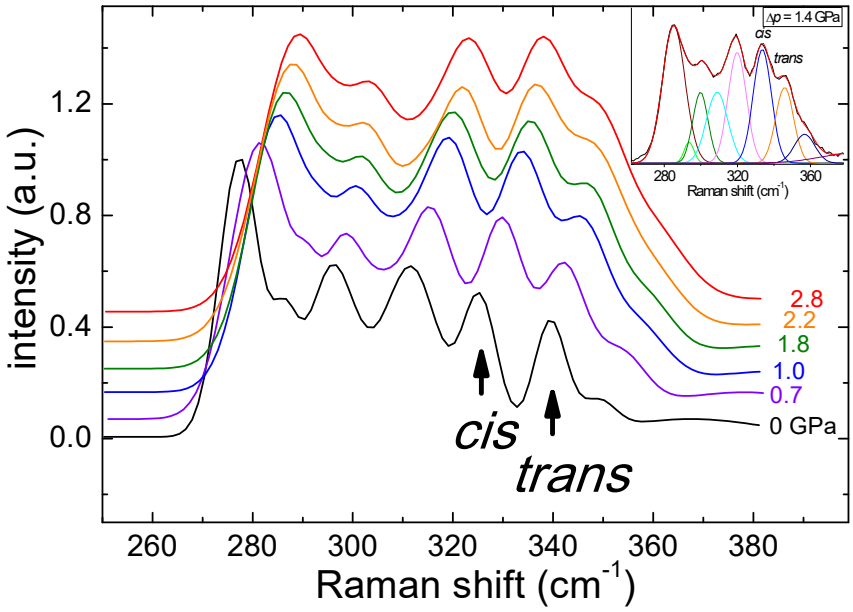

Fig. 9 Pressure dependence of the Raman spectrum between 250 and 400 cm^{-1}. The spectra are vertically shifted for clarity. In the inset an example of the quality of the fit is reported.

The evolution of the relative concentration of the conformers as a function of pressure is a useful tool to investigate their volume difference, ΔV. Indeed, the equilibrium constant between the conformers, *K*, depends on pressure according to the following expression:[37,38]

$$\left(\frac{\partial \ln K}{\partial p}\right)_T = -\frac{\Delta V}{RT}$$

where *R* is the gas constant and *T* is the absolute temperature at which measurements are conducted (300 K in the present case). Bearing in mind that $K \propto r$, where *r* is given by equation (1), one can obtain the difference of the volumes of the two conformers of TFSI as the slope of the best line fit of the graph of $\ln(r)$ vs. *p* (Fig. 10). Of course, as pressure

increases the concentration of the conformer with the lowest molecular volume increases. In the present case the experiments indicate that *cis*-TFSI has a smaller molecular value by $\Delta V = 0.34 \pm 0.02$ cm^3/mol, a value similar to that recently reported (0.41 ± 0.05 cm^3/mol) for a IL with TFSI as anion and an ammonium based cation.[39]

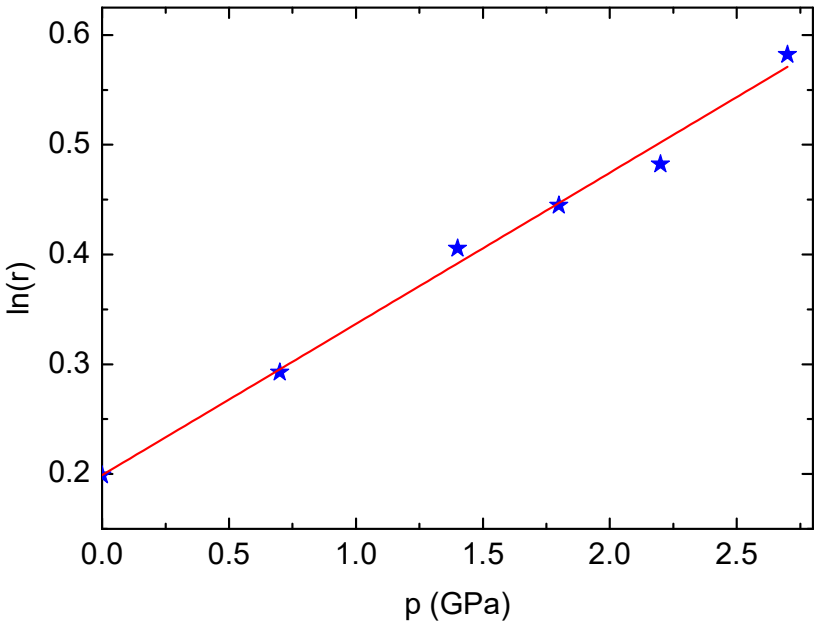

Fig. 10 Pressure dependence of ln(*r*) and best fit line.

Conclusions

The Raman spectrum of 1-butyl-1-methylpyrrolidinium bis(trifluoromethanesulfonyl)imide has been investigated as a function of temperature at ambient pressure. The visual inspection of the sample shows different morphologies for the two low temperature crystalline phases; moreover, in both of them only the *trans* conformer of TFSI is spectroscopically detected. The Raman study was also conducted at $T = 300$ K as a

function of pressure up to 8 GPa. The pressure dependence of both the line-shape behavior of the ruby fluorescence bands and the peak frequency of the most intense Raman band centered around 740 cm^{-1} indicate the occurrence of a sharp liquid-solid transition at about 2.2. GPa. The pressure behavior of the whole Raman spectrum, the comparison with the temperature dependence as well as the evolution of the low frequency Raman response which displays a hindered molecular motion with almost stuck molecules at high pressures, suggest the onset of a glassy phase in the high pressure regime. Finally, the present study indicates that the cisoid conformer of TFSI is preferred when pressure is applied as it possesses a smaller volume with respect to the transoid rotamer by about 0.34 ± 0.02 cm^3/mol. These findings thus provide a simple and clear link among the macroscopic phases of the ILs and the molecular configurations as well as an experimental benchmark for refining more accurate theoretical models.

References

(1) Matic, A.; Scrosati, B. Ionic Liquids for Energy Applications. *MRS Bull*. **2013**, *38*, 533-536.

(2) Vitucci, F. M.; Manzo, D.; Navarra, M. A.; Palumbo, O.; Trequattrini, F.; Panero, S.; Bruni, P.; Croce, F.; Paolone, A. Low-Temperature Phase Transitions of 1-Butyl-1-methylpyrrolidinium Bis(trifluoromethanesulfonyl)imide Swelling a Polyvinylidenefluoride Electrospun Membrane. *J. Phys. Chem. C* **2014**, *118*, 5749-5755.

(3) Yoshimura, Y.; Takekiyo, T.; Imai, Y.; Abe, H. Pressure-Induced Spectral Changes of Room-Temperature Ionic Liquid, N,N-Diethyl-N-methyl-N-(2-methoxyethyl)ammonium Bis(trifluoromethylsulfonyl)imide, (DEME)(TFSI). *J. Phys. Chem. C* **2012**, *116*, 2097–2101.

(4) Yoshimura, Y.; Abe, H.; Imai, Y.; Takekiyo, T.; Hamaya, N. Decompression-Induced Crystal Polymorphism in a Room-Temperature Ionic Liquid, N,N-Diethyl-N-methyl-N-(2-methoxyethyl) Ammonium Tetrafluoroborate. *J. Phys. Chem. B* **2013**, *117*, 3264−3269.

(5) Trequattrini, F.; Paolone, A.; Palumbo, O.; Vitucci, F.M.; Navarra, M. A.; Panero, S. Low Frequency Mechanical Spectroscopy Study of Three Pyrrolidinium Based Ionic Liquids. *Arch. Metall. Mater*. **2015**, *60*, 385-390.

(6) Mangialardo, S.; Baldassarre, L.; Bodo, E.; Postorino, P. in *The Structure of Ionic Liquids*, ed. by R. Caminiti and L. Gontrani, Springer International Publishing Switzerland 2014.

(7) Ribeiro M. C. C. Correlation between Quasielastic Raman Scattering and Configurational Entropy in an Ionic Liquid. *J. Phys. Chem. B* **2007**, *111*, 5008-5015.

(8) Heimer, N. E.; Del Sesto, R. E.; Meng, Z. Z.; Wilkes, J. S.; Carper, W. R. Vibrational Spectra of Imidazolium Tetrafluoroborate Ionic Liquids. *J. Mol. Liq.* **2006**, *124*, 84-95.

(9) Bodo, E.; Postorino, P.; Mangialardo, S.; Piacente, G.; Ramondo, F.; Bosi, F.; Ballirano, P.; Caminiti, R. Structure of the Molten Salt Methyl Ammonium Nitrate Explored by Experiments and Theory. *J. Phys. Chem. B* **2011**, *115*, 13149–13161.

(10) Bodo, E.; Sferrazza, A.; Caminiti, R.; Mangialardo, S.; Postorino, P. A Prototypical Ionic Liquid Explored by ab-initio Molecular Dynamics and Raman Spectroscopy. *J. Chem. Phys.* **2013**, *139*, 144309.

(11) Bodo, E.; Mangialardo, S.; Ramondo, F.; Ceccacci, F.; Postorino, P. Unravelling the Structure of Protic Ionic Liquids with Theoretical and Experimental Methods: Ethyl-, Propyl- and Butylammonium Nitrate Explored by Raman Spectroscopy and DFT Calculations. *J. Phys. Chem. B* **2012**, *116*, 13878−13888.

(12) Bodo, E.; Mangialardo, S.; Capitani, F.; Gontrani, L.; Leonelli, F.; Postorino, P. Interaction of a Long Alkyl Chain Protic Ionic Liquid and Water. *J. Chem. Phys.* **2014**, *140*, 204503.

(13) Martinelli, A.; Matic, A.; Johansson, P.; Jacobsson, P.; Borjesson, L.; Fernicola, A.; Scrosati, B.; Ohno, H. Conformational Evolution of TFSI− in Protic and Aprotic Ionic Liquids. *J. Raman Spectrosc*. **2011**, *42*, 522–528.

(14) Castriota, M.; Caruso, T.; Agostino, R. G.; Cazzanelli, E.; Henderson, W. A.; Passerini, S. Raman Investigation of the Ionic Liquid N-Methyl-N-propylpyrrolidinium Bis(trifluoromethanesulfonyl)imide and Its Mixture with $LiN(SO_2CF_3)_2$. *J. Phys. Chem. A* **2005**, *109*, 92-96.

(15) Vitucci, F. M.; Trequattrini, F.; Palumbo, O.; Brubach, J.-B.; Roy, P.; Paolone, A. Infrared Spectra of Bis(trifluoromethanesulfonyl)imide Based Ionic Liquids: Experiments and DFT Simulations. *Vib. Spec*. **2014**, *74*, 81–87.

(16) Ribeiro, M. C. C. Low-frequency Raman Spectra and Fragility of Imidazolium Ionic Liquids. *J. Chem. Phys.* **2010**, *133*, 024503.

(17) Iwata, K. I.; Okajima, H.; Saha, S.; Hamagouchi, H. Local Structure Formation in Alkyl-imidazolium-Based Ionic Liquids as Revealed by Linear and Nonlinear Raman Spectroscopy. *Acc. Chem. Res.* **2007,** *40,* 1174–1181.

(18) Ribeiro, M. C. C.; Pádua, A. A. H.; Costa Gomes, M. F. Glass Transition of Ionic Liquids Under High Pressure. *J. Chem. Phys*. **2014**, *140*, 244514.

(19) Imai, Y.; Takekiyo, T.; Abe, H.; Yoshimura, Y. Pressure- and Temperature-Induced Raman Spectral Changes of 1-Butyl-3-methylimidazolium Tetrafluoroborate. *High Pressure Res*. **2010**, *31*, 53-57.

(20) Takekiyo, T.; Imai, Y.; Hatano, N.; Abe, H.; Yoshimura, Y. Pressure-Induced Phase Transition of 1-Butyl-3-methylimidazolium Hexafluorophosphate (bmim)(PF_6). *High Pressure Res.* **2010**, *31*, 35-38.

(21) Russina, O.; Fazio, B.; Schmidt, C.; Triolo, A. Structural Organization and Phase Behaviour of 1-Butyl-3-methylimidazolium Hexafluorophosphate: an High Pressure Raman Spectroscopy Study. *Phys. Chem. Chem. Phys.* **2011**, *13*, 12067-12074.

(22) Su, L.; Li, M.; Zhu, X.; Wang, Z.; Chen, Z.; Li, F.; Zhou, Q.; Hong, S. In Situ Crystallization of Low-Melting Ionic Liquid (BMIM)(PF_6) under High Pressure up to 2 GPa. *J. Phys. Chem. B* **2010**, *114*, 5061-5065.

(23) Faria, L. F. O.; Nobrega, M. M.; Temperini, M. L. A.; Ribeiro, M. C. C. Ionic Liquids Based on the bis(trifluoromethylsulfonyl)imide Anion for High-Pressure Raman Spectroscopy Measurements. *J. Raman Spectrosc.* **2013**, *44*, 481–484.

(24) Glebov, A. L.; Mokhun, O.; Rapaport, A.; Vergnole, S.; Smirnov, V.; Glebov, L. B. Volume Bragg Gratings as Ultra-narrow and Multiband Optical Filters. *Proc. SPIE 8428, Micro-Optics 2012*, **2012**, 84280C.

(25) Capitani, F.; Fasolato, C.; Mangialardo, S.; Signorelli, Sa.; Gontranic, L.; Postorino, P. Heterogeneity of Propyl-Ammonium Nitrate Solid Phases Obtained Under High Pressure. *J. Phys. Chem. Sol.* **2015**, *84*,13-16.

(26) Capitani, F.; Koval, S.; Fittipaldi, R.; Caramazza, S.; Paris, E.; Mohamed, W. S.; Lorenzana, J.; Nucara, A.; Rocco, L.; Vecchione, A.; Postorino, P.; Calvani, P. Raman Phonon Spectrum of the Dzyaloshinskii-Moriya Helimagnet $Ba_2CuGe_2O_7$. *Phys. Rev. B* **2015**, *91*, 214308.

(27) Zardo, I.; Yazji, S.; Marini, C.; Uccelli, E.; Fontcuberta i Morral, A.; Abstreiter, G.; Postorino, P. Pressure Tuning of the Optical Properties of GaAs Nanowires. *ACS Nano* **2012**, *6*, 3284–3291.

(28) Herstedt, M.; Smirnov, M.; Johansson, P.; Chami, M.; Grondin, J.; Servant, L.; Lassègues, J. C. Spectroscopic Characterization of the Conformational States of the Bis(trifluoromethanesulfonyl)imide Anion (TFSI−). *J. Raman Spectrosc.* **2005**, *36*, 762-770.

(29) Fujimori, T.; Fujii, K.; Kanzaki, R.; Chiba, K.; Yamamoto, H.; Umebayashi, Y.; Ishiguro, S.-I. Conformational Structure of Room Temperature Ionic Liquid N-butyl-N-methyl-pyrrolidinium bis(trifluoromethanesulfonyl) Imide — Raman Spectroscopic Study and DFT Calculations. *J. Mol. Liq.* **2007**, *131-132*, 216-224.

(30) Canongia Lopes, J. N.; Shimizu, K.; Pádua, A. A. H.; Umebayashi, Y.; Fukuda, S.; Fujii, K.; Ishiguro, S.-I. A Tale of Two Ions: The Conformational Landscapes of Bis(trifluoromethanesulfonyl)amide and N,N-Dialkylpyrrolidinium. *J. Phys. Chem. B* **2008**, *112*, 1465-1472.

(31) Choudury, A. R.; Winterton, N.; Steiner, A.; Cooper, A. I.; Johnson, K. A. In situ Crystallization of Low-Melting Ionic Liquids. *J. Am. Chem. Soc*. **2005**, *127*, 16792-16793.

(32) Vitucci, F. M.; Palumbo, O.; Trequattrini, F.; Brubach, J.-B.; Roy, P.; Meschini, I.; Croce, F.; Paolone, A. Interaction of 1-Butyl-1-methylpyrrolidinium Bis(trifluoromethanesulfonyl)imide with an Electrospun PVdF Membrane: Temperature Dependence of the Concentration of the Anion Conformers *J. Chem. Phys.* **2015**, *143*, 094707.

(33) Vitucci, F. M.; Trequattrini, F.; Palumbo, O.; Brubach, J.-B.; Roy, P.; Navarra, M. A.; Panero, S.; Paolone, A. Stabilization of Different Conformers of Bis(trifluoromethanesulfonyl)imide Anion in Ammonium-Based Ionic Liquids at Low Temperatures. *J. Phys. Chem. A* **2014**, *118*, 8758−8764.

(34) Piermarini, G. J.; Block S.; Barnett, J. D. Hydrostatic Limits in Liquids and Solids to 100 kbar. *J. Appl. Phys*. **1973**, *44*, 5377-5382.

(35) Munro, R. G.; Block, S.; Piermarini, G. J. Correlation of the Glass Transition and the Pressure Dependence of Viscosity in Liquids. *J. App. Phys*. **1979**, *50*, 6779-6783.

(36) Fanetti, S.; Citroni, M.; Bini, R. Pressure-Induced Fluorescence of Pyridine. *J. Phys. Chem. B* **2011**, *115*, 12051-12058.

(37) Takekiyo T.; Yoshimura, Y. Raman Spectroscopic Study on the Hydration Structures of Tetraethylammonium Cation in Water. *J. Phys. Chem. A* **2006**, *110*, 10829-10833.

(38) Takekiyo, T.; Kato, M.; Taniguchi, Y. Pressure Effect on Conformational Equilibria of Analog Peptides in Aqueous Solution by Raman Spectroscopy. *J. Solution Chem*. **2004**, *33*, 761-775.

(39) Capitani, F.; Gatto, S.; Postorino, P.; Palumbo, O.; Trequattrini, F.; Deutsch, M.; Brubach, J.-B.; Roy, P.; Paolone, A. The Complex Dance of the Two Conformers of Bis(trifluoromethanesulfonyl)imide as a Function of Pressure and Temperature. *J. Phys. Chem. B*. DOI: 10.1021/acs.jpcb.5b12537.

Table of Content